10th Canadian Masonry Symposium, Banff, Alberta, June 8 – 12, 2005

# MATERIAL MODEL FOR UNREINFORCED MASONRY BASED ON PLASTICITY THEORY

**S. Lu[1], R. Heuer[2], R. Flesch[3]**

[1]Dipl.-Ing., Scientist, Business Unit Transport Routes Engineering, **arsenal research**, Faradaygasse 3, 1030 Vienna, Austria, suikai.lu@arsenal.ac.at

[2]Professor, CMSD – Center of Mechanics and Structural Dynamics, **Vienna University of Technology** Wiedner Hauptstraße 8 / 2063, 1040 Vienna, Austria, rh@allmech.tuwien.ac.at

[3]Professor, Head of Business Unit, Business Unit Transport Routes Engineering, **arsenal research**, Faradaygasse 3, 1030 Vienna, Austria, rainer.flesch@arsenal.ac.at

## ABSTRACT

This paper presents a new model for unreinforced masonry (URM), based on the plastic material model by Ganz [1]. The general idea is to use a combination of yielding surfaces in stress space, where each surface captures one failure mode. Compared to the material model of Ganz [1], the new model was extended to cover even the tension strength aspects of masonry constructions in both directions (in plane, orthogonal and parallel to the horizontal joints) for each failure mode. The model consists of only 5 convex yielding surfaces which describe the following failures, respectively:

-) tension failure
-) compression failure
-) shear failure
-) sliding along the horizontal joints
-) tension failure in the horizontal joints

In addition to the theoretical background, an application is shown where laboratory experiments are used to test and calibrate the material model and its parameters. Therefore, this model was implemented into the Finite Element Software ANSYS. The implementation involves all failure modes and an automatic search for the positions of the masonry structures in the global FE-model. The result of this numerical implementation is a display of the cracked and yielded areas of the wall, respectively. The accuracy depends on the size of the finite elements chosen in the model.

**KEYWORDS**: URM, material model, macro model, plasticity theory, finite element method, ANSYS

## INTRODUCTION

Based on the classic theory of plasticity, Ganz [1] formulated two material models in 1985, where he described yielding surfaces for each failure mode in masonry. First he formulated a model for URM, which covers only 5 yielding surfaces. Then he developed a model including tension strength aspects, where 12 surfaces were needed. The new model, presented in this paper, extends the basic Ganz-model (without tension strength) by including tension in a new effective approach capturing the main failure modes of unreinforced masonry structures.

Both the analytical derivations as well as the main result of this research work, the software implementation in form of a macro for the FE Software ANSYS are presented.

To verify the model, experimental laboratory tests will be analyzed numerically using this macro-model, to confirm and prove the analytical work. In the last part of this paper, numerical and experimental results are compared to each other in Table 2.

## ORIGINAL MODEL BY GANZ [1]

In 1985, Ganz [1] formulated a material model for URM, where the two components brick and joints were split.

### Failure in the Brick

For the component brick, he focused on the most general form, perforated bricks (see Figure 1). Within a limiting approach this theory also can be applied to a solid brick.

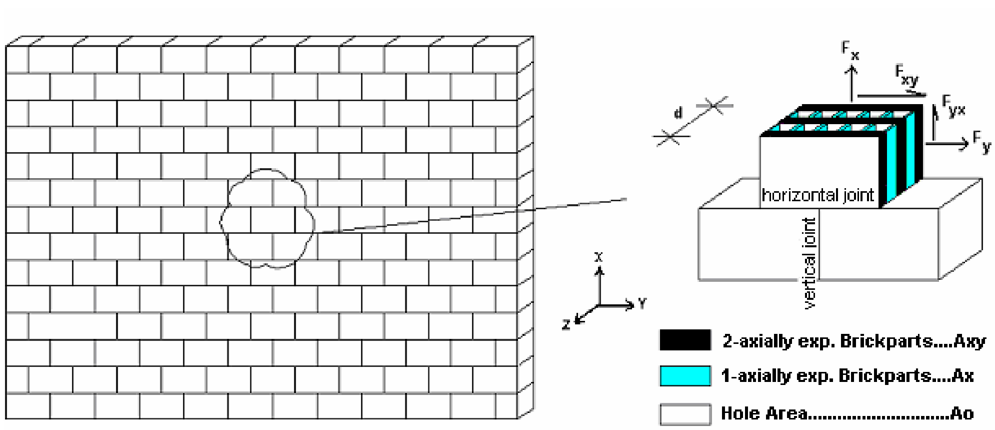


**Figure 1 – Brick Element**

The considered forces and cross sections are defined as follows:

$$F_x = F_{x,1} + F_{x,2} \qquad \text{Equation 1}$$

$F_x$ stands for the normal force, and $F_{x,1}$, $F_{x,2}$ act upon $A_x$, $A_{xy}$, respectively.

$$F_y = F_{y,1} + F_{y,2} \qquad \text{Equation 2}$$

$F_y$ stands for the horizontal force, and $F_{y,1}$, $F_{y,2}$ act upon $A_x$, $A_{xy}$, respectively.

$$F_{xy} = F_{xy,1} + F_{xy,2} \qquad \text{Equation 3}$$

$F_{xy}$ stands for the shear force, and $F_{xy,1}$, $F_{xy,2}$ act upon $A_x$, $A_{xy}$ respectively. The total cross sectional area reads

$$A = A_x + A_{xy} + A_0$$ Equation 4

By combining the uni- and biaxial parts of the forces using principal forces, the following three equations result for failure in the brick:

$$f_1 = \tau_{xy}^2 - \sigma_x \sigma_y \leq 0$$ tension failure in brick Equation 5

$$f_2 = \tau_{xy}^2 - (\sigma_x + f_{cx})(\sigma_y + f_{cy}) \leq 0$$ compression failure in brick Equation 6

$$f_3 = \tau_{xy}^2 + \sigma_y (\sigma_y + f_{cy}) \leq 0$$ shear failure in brick Equation 7

**Failure in the Mortar**
Supposing that the vertical joints are not filled, it is only necessary to focus on the horizontal joints. With this assumption the model equations are on the "conservative side".

Sliding in the joints is modeled by means of the Mohr-Coulomb law,

$$f_4 = \tau_{xy}^2 - (c - \sigma_x \tan(\varphi))^2 \leq 0$$ sliding along the horizontal joints Equation 8

Finally, a tension cut-off for the Mohr Coulomb friction law is formulated,

$$f_5 = \tau_{xy}^2 + \sigma_x \left[ \sigma_x + 2c \tan(\frac{\pi}{4} + \frac{\varphi}{2}) \right] \leq 0$$ tension failure in the horizontal joints Equation 9

Equation 5 to Equation 9 describe the law for URM according to Ganz considering the components of compressive strength $f_{cx}$, $f_{cy}$, respectively.

**MODIFIED MODEL**

**Failure in the Brick**
The new model, developed within this research work, was expanded to consider tension stresses. Taking the uniaxial exposed parts of the brick section, the governing equations can be written as:

$$\beta_t A_x \geq F_{x,1} \geq -\beta_c A_x$$ Equation 10

$$F_{y,1} \equiv F_{xy,1} \equiv 0$$ Equation 11

where $\beta_c$, $\beta_t$ denote compression strength and tension strength of brick, respectively.

For the biaxially exposed parts, the inequality can be written by using the principal forces in terms of

$$\beta_t A_{xy} \geq F_{1,2} = \frac{(F_{x,2} + F_{y,2})}{2} \pm \sqrt{\left(\frac{F_{x,2} - F_{y,2}}{2}\right)^2 + F_{xy,2}^2} \geq -\beta_c A_{xy}$$ Equation 12

Combining Equation 10 to Equation 12 and by substitution of

$$\beta_t (\frac{A_{xy} + A_x}{A}) = f_{tx} \ , \qquad \beta_t \frac{A_{xy}}{A} = f_{ty}$$ Equation 13

the former material laws derived for brick (Equations 5 and 7) can be replaced by

$$f_1 = \tau_{xy}^2 - (\sigma_x - f_{tx})(\sigma_y - f_{ty}) \leq 0$$ Equation 14

$$f_3 = \tau_{xy}^2 + \sigma_y \left(f_{cy} - f_{ty} + \sigma_y\right) - f_{cy} f_{ty} \leq 0$$ Equation 15

The surface function $f_2$ (Equation 6) remains unchanged.

**Failure in the Mortar**

To enclose tension in joints, criteria $f_4$ (Equation 8) can also remain unchanged, but the equation for tension cut-off $f_5$ (Equation 9) has to be modified (Figure 2).

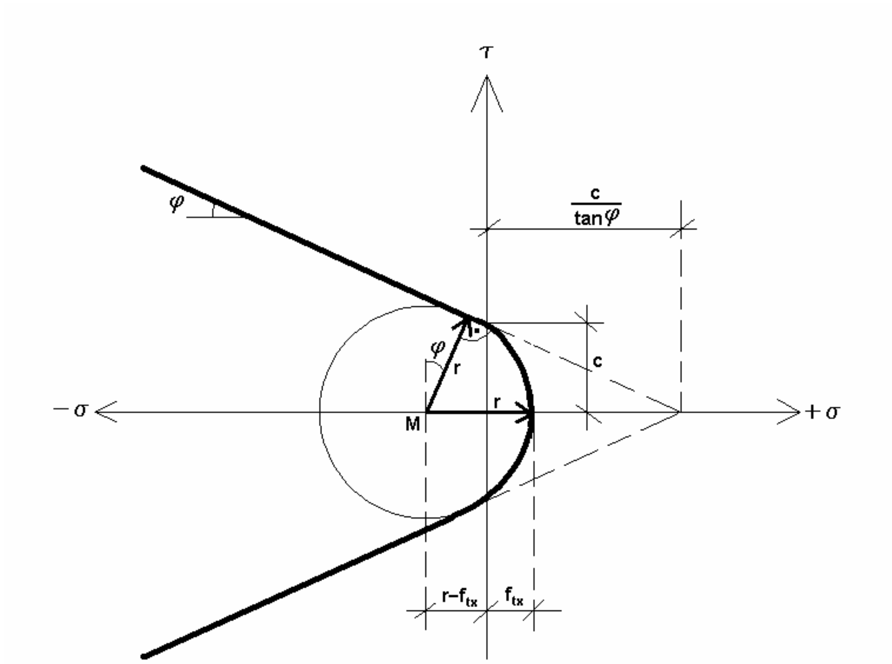


**Figure 2 – Tension cut-off**

Finally, $f_5$ can be written in terms of

$$f_5 = \tau_{xy}^2 + {\sigma_x}^2 + 2\frac{c \cdot \cos\varphi - \sin\varphi \cdot f_{tx}}{1 - \sin\varphi}(\sigma_x - f_{tx}) - 2\sigma_x f_{tx} + {f_{tx}}^2 \leq 0$$ Equation 16

The new material model (Equation 14, 6, 15, 8, 16) can be graphically displayed as a combined yielding surface (Figure 3):

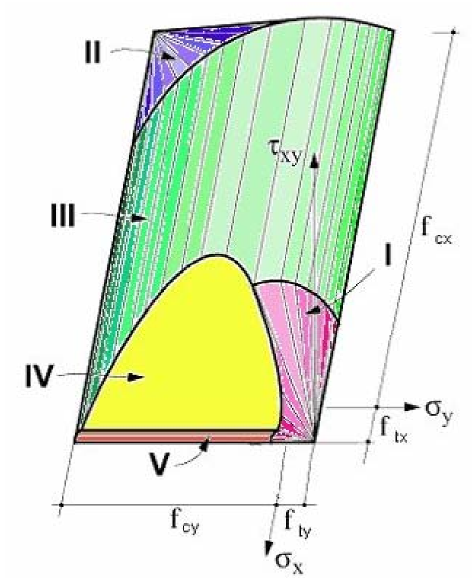


**Figure 3 – Combined Yielding Surface of the extended model for URM**

The described failures of the five yielding surfaces can be interpreted in the same way as the original model by Ganz (compare previous section).

## INPUT URM PARAMATERS FOR ANALYTICAL ANALYSIS

For numerical implementation of the URM model, some main input parameters are necessary. The following section presents an overview of the data evaluation used for the analysis.

**Compression strength orthogonal to the horizontal joints [2]:** $f_{cx}$

$$f_{cx} = K \cdot \beta_c^{0.75} \cdot f_{mc}^{0.25} \qquad \text{Equation 17}$$

with the coefficient $K = 1.0 \div 1.5$, and the compression strength of the considered mortar $f_{mc}$.

**Compression strength parallel to the horizontal joints [3]:** $f_{cy}$

URM consisting of solid brick:

$$f_{cy} = 0.75 \cdot f_{cx} \qquad \text{Equation 18}$$

URM consisting of perforated brick:

$$f_{cy} = 0.5 \cdot f_{cx} \qquad \text{Equation 19}$$

**Tension strength orthogonal to the horizontal joints [4]:** $f_{tx}$

The tension strength of URM only depends on the tension strength of the used mortar $f_{mt}$ and can be written as:

$$f_{tx} = \frac{2}{3} \cdot f_{mt} \quad \text{Equation 20}$$

**Tension strength parallel to the horizontal joints [5]:** $f_{ty}$

In the case of tension strength parallel to the horizontal joints, two different crack types should be treated separately. Crack Type A (Figure 4) occurs if bricks are made of low quality materials and if large portions of the normal stresses $\sigma_x$ are exposed to masonry members.

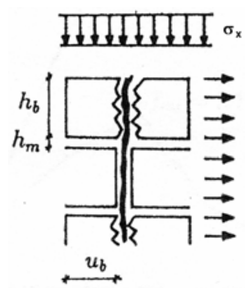


**Figure 4 – Crack Type A, taken from [6]**

$$f_{ty,CT\_A} = \frac{f_{tbm} + f_{bt,horiz}}{2(1+\alpha)} + \frac{f_{mt}}{1+\frac{1}{\alpha}} \quad \text{Equation 21}$$

where $\alpha = \frac{h_m}{h_b}$, $f_{bt,horiz}$ denotes the horizontal tension strength of the brick used, and $f_{tbm}$ is the adhesive tensile strength between the mortar and the brick.

Crack Type B (Figure 5) is typical for high strength bricks in combination with low quality mortar and/or if the exposing normal stress $\sigma_x$ is very small.

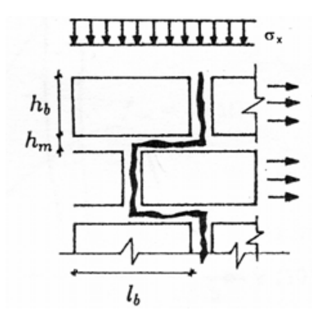


**Figure 5 – Crack Type B, taken from [6]**

$$f_{ty,CT\_B} = \frac{f_{tbm}}{1+\alpha} + \frac{f_{mt}}{1+\frac{1}{\alpha}} + \beta \frac{f_{sbm}}{2(1+\alpha)} \quad \text{Equation 22}$$

where $f_{sbm}$ stands for the adhesive shear strength between the mortar and the brick, and the coefficient $\beta$ describes the ratio $\beta = \frac{l_b}{h_b}$.

**Young's modulus orthogonal to the horizontal joints [2]: $E_x$**

$$E_x = 1000 \cdot f_{cx} \qquad \text{Equation 23}$$

**Young's modulus parallel to the horizontal joints [7, 8]: $E_Y$**

$$E_Y = \frac{E_X}{1 + 2 \cdot \pi \cdot f} \qquad \text{Equation 24}$$

where $f \approx \frac{h_b}{4 \cdot l_b}$.

**Friction angle: $\varphi$; and shear strength under no compressive stress: c**

The Friction angle $\varphi$ varies normally between 20° and 40°, and the shear strength under zero compressive stress is between 0.2 – 2.5 MPa where some numbers for c are listed in Table 3.4 of the Euro Code [2].

**IMPLEMENTATION OF THE NEW MODEL INTO THE FE-SOFTWARE ANSYS**

To implement the model into FE-software, it should be taken into account, that

$$f_{tx} \leq \frac{c}{\tan \varphi}. \qquad \text{Equation 25}$$

If this condition is not maintained, $f_{tx}$ has to be set equal to $\frac{c}{\tan \varphi}$, before continuing the analysis. The stress state of the object analyzed must be verified. Four different positions can be distinguished (Figure 6). Therefore, an extra condition, Equation 26, has to be considered.

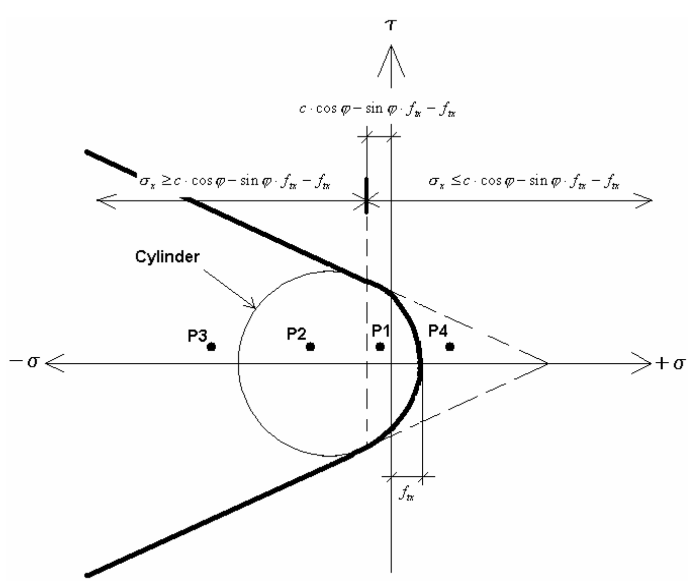


**Figure 6 – Positions of the analyzed stress state**

$$f_{5/T2} = c \cdot \cos\varphi - \sin\varphi \cdot f_{tx} - f_{tx} + \sigma_x \quad \begin{matrix} \geq 0 \ \ then \ \ the \ \ result \ \ is \ \ 1 \\ < 0 \ \ then \ \ the \ \ result \ \ is \ \ 0 \end{matrix}$$

Equation 26

Together with condition $f_5$,

$$f_5 = \tau_{xy}^2 + {\sigma_x}^2 + 2\frac{c \cdot \cos\varphi - \sin\varphi \cdot f_{tx}}{1 - \sin\varphi}(\sigma_x - f_{tx}) - 2\sigma_x f_{tx} + {f_{tx}}^2 \quad \begin{matrix} \leq 0 \ \ then \ \ the \ \ result \ \ is \ \ 0 \\ > 0 \ \ then \ \ the \ \ result \ \ is \ \ 1 \end{matrix},$$

Equation 27

the four positions can be separated numerically in the following way:

P1: $f_5 \cdot f_{5/T2} = 0 \cdot 1 = 0$;P2: $f_5 \cdot f_{5/T2} = 0 \cdot 0 = 0$;P3: $f_5 \cdot f_{5/T2} = 1 \cdot 0 = 0$;P4 $f_5 \cdot f_{5/T2} = 1 \cdot 1 = 1$

Equation 28

Only in case of P4 is the analyzed stress point outside the combined yielding surface, which means that cracks will occur. The combined yielding surface was implemented into ANSYS (Figure 7) including the conditions described previously.

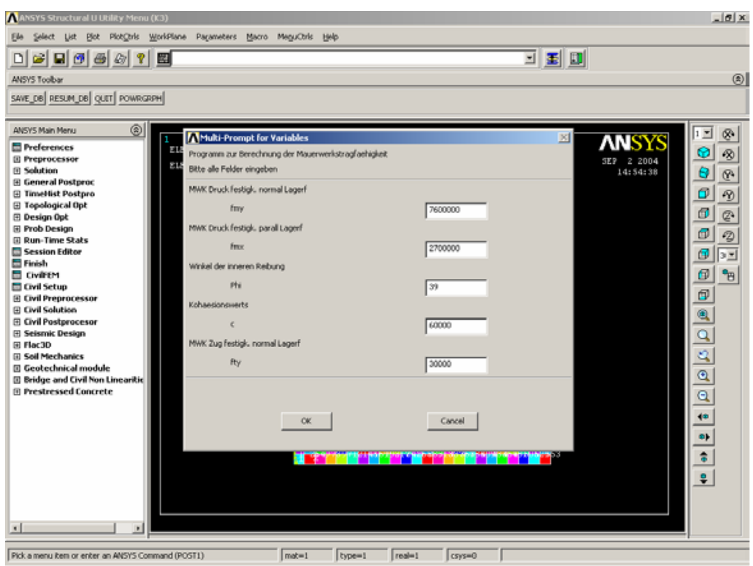


**Figure 7 – Screenshot of the implemented Program for URM**

The implementation also involves an automatic detection of the positions of the masonry structures in the global FE-model.

## VERIFICATION OF THE MATERIAL MODEL BY NUMERICAL ANALYSIS OF LABORATORY TESTS

In 1982, Ganz et al. [9] performed experimental tests on URM. They tested the specimens stepwise until they collapsed. Those tested walls were subjected either to uniaxial and/or biaxial loading. Also the angle of the horizontal joints of each specimen varied between 0; 22.5; 45; 67.5 and 90 degrees.

To verify the material model and to demonstrate the implemented macro-model, these experimental tests have been recalculated numerically and were compared to the test results.

Input data for the computer simulation are given in Table 1.

**Table 1 – Input data for computer simulation**

| | | | |
|---|---|---|---|
| **Density** | ρ | (kg/m³) | 905 |
| **Strengths** | $f_{cx}$ | (N/mm²) | 7.6 |
| | $f_{cy}$ | (N/mm²) | 2.7 |
| | $f_{tx}$ | (N/mm²) | 0.03 |
| | $f_{ty}$ | (N/mm²) | 0.00 |
| **Cohesion** | c | (N/mm²) | 0.06 |
| **Friction angle** | $\varphi$ | (°) | 39 |

In Figure 8, K3 of the test series is displayed graphically, to show the effectiveness of the implementation.

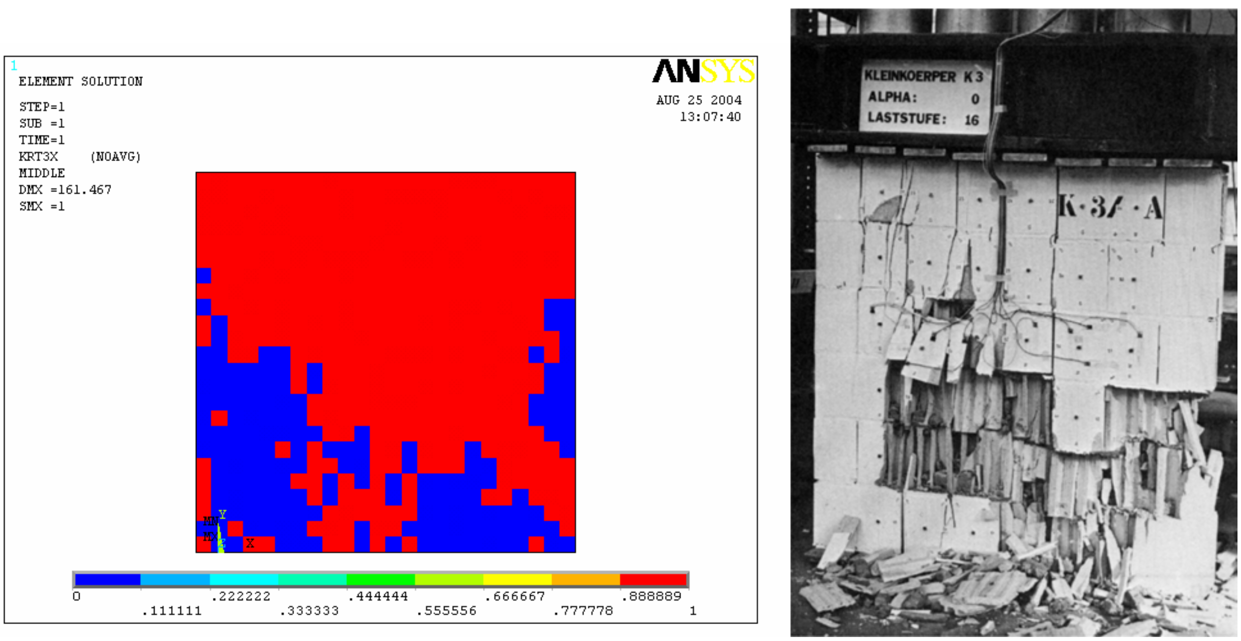


**Figure 8 – left: numerical implementation; right: laboratory experiment on real test specimen**

A summary of additional results is given in Table 2, where stresses were measured in the middle of the wall and were taken from the middle element of the FE-Model. There is good agreement.

**Table 2 – Comparison between test results and numerically analyzed results**

| Test | Angle of horiz. joints | Ratio $F_H / F_V$ | Measured $\sigma_{crack}$ at laboratory (taken from [9]) | | | Numerically analyzed $\sigma_{crack}$ | | |
|---|---|---|---|---|---|---|---|---|
| | | | $\sigma_X$ | $\sigma_Y$ | $\tau_{XY}$ | $\sigma_X$ | $\sigma_Y$ | $\tau_{XY}$ |
| | (°) | | (N/m²) | (N/m²) | (N/m²) | (N/m²) | (N/m²) | (N/m²) |
| **K1** | 22.5 | 1 / -10.9 | -8.00 e4 | -9.20 e5 | 4.20 e5 | -7.89e4 | -9.10e5 | 4.14e5 |
| **K3** | 0.0 | 0 / -1 | 0 | -7.63 e6 | 0 | 0 | 7.61e6 | 0 |
| **K4** | 90.0 | 0 / -1 | -1.83 e6 | 0 | 0 | -2.70e6 | 0 | 0 |
| **K6** | 45.0 | 0 / -1 | -3.20 e5 | -3.20 e5 | 3.20 e5 | -3.19e5 | -3.19e5 | 3.19e5 |
| **K7** | 22.5 | 0 / -1 | -3.90 e5 | -2.25 e6 | 9.30 e5 | -3.99e5 | -2.33e6 | 9.64e5 |
| **K8** | 67.5 | 0 / -1 | -2.20 e5 | -4.00 e4 | 9.00 e4 | -2.28e5 | -3.91e4 | 9.43e4 |
| **K10** | 0.0 | -1 / -3.2 | -2.11 e6 | -6.44 e6 | 0 | -2.40e6 | -7.3e6 | 0 |
| **K11** | 22.5 | -1 / -3.1 | -2.04 e6 | -4.49 e6 | 1.23 e6 | -2.07e6 | -4.36e6 | -1.13e6 |
| **K12** | 45.0 | -1 / -3.2 | -2.03 e6 | -2.03 e6 | 1.08 e6 | -2.05e6 | -2.05 e6 | -1.05e6 |


## ACKNOWLEDGEMENTS

The research work of this paper was funded by arsenal research (Fund No: 2.05.00187.4.0). The authors are grateful for this support and want to thank them.


## REFERENCES


1. Ganz, H. R., Mauerwerksscheiben unter Normalkraft und Schub. Institut für Baustatik und Konstruktion, ETH Zurich, report no. 148, 1985.
2. Code, EN 1996-1-1, Design of Masonry Structures, part 1-1 common rules for reinforced and unreinforced masonry structures.
3. Glitzka, H., Druckbeanspruchung parallel zur Lagerfuge. Mauerwerkskalender 1988, pp 489 – 496, Ernst & Sohn, 1988.
4. Tassios, Εργαστηριο Ωπλισμενον Σκνροδεματοζ, Η Μηχανικη, τηζ, τοιχοποιιαζ. Αθηνα, 1986.
5. Drysdale, R.G., Hamid, A. A., Tensile strength of brick masonry. Int. Journal of Masonry Construction, Vol.2, No.4, 1982.
6. Vratsanou, V., Das nichtlineare Verhalten unbewehrter Mauerwerksscheiben unter Erdbebenbeanspruchung. Ph. D. Thesis, Institut für Massivbau und Baustofftechnologie, Universität Fridericiana zu Karlsruhe TH, 1992.
7. Graubner, C. A., Glock, C., Meyer, G., Abschätzung der Knicklänge mehrseitig gehaltener Wände aus großformatigen Mauersteinen. Bauingenieur, Juni 2004, pp 300-305, Springer, 2004.
8. Gross, D., Seelig, T., Bruchmechanik mit einer Einführung in die Mikromechanik. 3. edt, Springer, 2001.
9. Ganz, H. R., Thürlimann, B., Versuche über die Festigkeit von zweiachsig beanspruchtem Mauerwerk. Institut für Baustatik und Konstruktion, ETH Zurich, report no. 7502-3, 1982.